

# Implementation of Single–Qutrit Quantum Gates via Tripod Adiabatic Passage

R. Nader-Ali, A. Jafari Dolama, and M. Amniat-Talab

Department of Physics, Faculty of Sciences, Urmia University, P.B. 165, Urmia, Iran.

**Abstract-** We proposed and analyzed implementation of the single-qutrit quantum gates based on stimulated Raman adiabatic passage (STIRAP) between magnetic sublevels in atoms coupled by pulsed laser fields. This technique requires only the control of the relative phase of the driving fields but do not involve any dynamical or geometrical phases, which make it independent of the other interaction details: detuning and pulse shapes, areas and durations. The suggested techniques are immune to spontaneous emission since the qubit and qutrit manipulation proceeds through non-absorbing dark states. In this paper, taking proper timing of the Rabi frequencies allows us to transfer the population of the system to a desired superposition of the ground states with the highest fidelity. We also obtained and implemented single-qutrit unitary gates, for transferring of the population of the system with different initial and final states.

**KEYWORDS:** STIRAP, Quantum gate, Adiabatic passage, Tripod, Geometric phases.

## I. INTRODUCTION

Quantum information processing requires the construction of specific quantum gates in a controllable way [1]. The growing interest in quantum computation stimulates the search for schemes to prepare and manipulate quantum states [2]. The physical implementation of the quantum computer is based on qubits quantum systems, which like the classical logical bits, have two states:  $|0\rangle$  and  $|1\rangle$  written in Dirac notation and known as computational basis states. Qutrits represent a very promising alternative to qubits for quantum information processing, because of their greater capability to encode and store more information [3, 4]. This reduces significantly the number of particles that need to be stored and

manipulated for quantum computing. The most natural physical candidate for representing a qutrit is the degenerate substates of an atomic energy level. It is therefore important to describe and analyze the dynamics of a quantum system which has an three degenerate ground level consisting of the  $|1\rangle, |2\rangle, |3\rangle$ , forming the qutrit, coupled to one excited state,  $|4\rangle$  [5].

A quantum gate is a unitary operator acting on the states of a certain set of qubits. If the number of such qubits is to be  $n$ , the quantum gate is represented by a  $2^n \times 2^n$  matrix in the unitary group  $U(2^n)$  [6]. Therefore the quantum single-qutrit gate is represented by a  $3 \times 3$  matrix in the unitary group  $U(3)$ .

The technique of stimulated Raman adiabatic passage (STIRAP) uses the coherence of two pulsed laser fields to achieve a complete population transfer from an initially populated ground state to a target ground state via an intermediate excited state [7]. In this configuration one assumes that the ground states are metastable, i.e., with negligible spontaneous emission in the considered time scale. The excited state has a relatively short lifetime of spontaneous emission. Instead of applying the pulses in the intuitive sequence, where the pump pulse (linking the initial populated ground state and the excited state) precedes the Stokes pulse (linking the excited state and the initially unpopulated ground state), the Stokes pulse precedes the pump pulse (as the so called counterintuitive pulse ordering). If the condition of two-photon resonance is satisfied, if there is sufficient overlap of the two pulse, and if the pulses are sufficiently strong such that the time evolution is adiabatic, then the complete population

transfer occurs between the ground states, without populating the intermediate excited state.

The tripod STIRAP technique, first proposed by Unanyan *et al.* [8,9], is an extension of STIRAP in which a third laser pulse (the control) couples the excited state to a fourth ground state. For a proper sequence of pump, Stokes, and control pulses, tripod STIRAP allows to create not only a coherent superposition of ground states, but also to construct coherently single-qutrit gates in the subspace of three ground states. In this paper, we use STIRAP technique for implementation of single-qutrit quantum gates. We propose a robust scheme that allows one to design quantum gates based on non-Abelian geometric phases without fragile dynamical phase. Finally we present the numeric corresponding to our schemes.

## II. CONSTRUCTION OF THE EFFECTIVE HAMILTONIAN

The linkage pattern of the tripod system is shown in Fig 1. The Hamiltonian of this system in the rotating-wave approximation can be written as (with  $\hbar = 1$ ):

$$H = \begin{pmatrix} 0 & 0 & 0 & \Omega_1(t)e^{+i(\alpha+\theta_1)} \\ 0 & 0 & 0 & \Omega_2(t)e^{+i(\alpha+\theta_2)} \\ 0 & 0 & 0 & \Omega_3(t)e^{+i(\alpha+\theta_3)} \\ \Omega_1(t)e^{-i(\alpha+\theta_1)} & \Omega_2(t)e^{-i(\alpha+\theta_2)} & \Omega_3(t)e^{-i(\alpha+\theta_3)} & \omega_4 \end{pmatrix} \quad (1)$$

where, the energy of the ground states  $|1\rangle, |2\rangle, |3\rangle$  is taken as zero,  $\Omega_i(t) = -\mu\epsilon_i(t)$ ,  $i = 1, 2, 3$  are the Rabi frequencies of the laser pulses, and  $\omega$ ,  $\theta_i$  are the carrier frequency and the initial phases of the laser pulses, respectively.

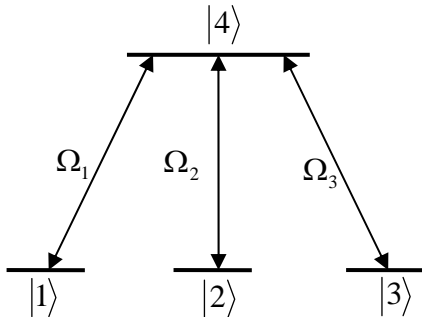


**Fig. 1** Linkage pattern of the system.

In the resonant case,  $\omega_4 = \omega$ , the effective Hamiltonian of the system is obtained by applying the unitary transformation on  $H$ ,

$$H^{eff}(t) = R^\dagger H R - i R^\dagger \frac{\partial R}{\partial t} \quad (2)$$

$$H^{eff}(t) = \frac{1}{2} \begin{pmatrix} 0 & 0 & 0 & \Omega_1(t) \\ 0 & 0 & 0 & \Omega_2(t) \\ 0 & 0 & 0 & \Omega_3(t) \\ \Omega_1(t) & \Omega_2(t) & \Omega_3(t) & 0 \end{pmatrix}$$

where the unitary transformation matrix  $R(t)$  is defined as:

$$R(t) = \begin{pmatrix} 1 & 0 & 0 & 0 \\ 0 & e^{-i(\theta_1-\theta_2)} & 0 & 0 \\ 0 & 0 & e^{-i(\theta_1-\theta_3)} & 0 \\ 0 & 0 & 0 & e^{-i(\omega t+\theta_1)} \end{pmatrix} \quad (3)$$

The corresponding dynamics of  $H^{eff}(t)$  is given by  $i \frac{\partial}{\partial t} |\Phi(t)\rangle = H^{eff}(t) |\Phi(t)\rangle$ . The relation between the state vector  $|\Psi(t)\rangle$  corresponding to  $H(t)$ , and the state vector  $|\Phi(t)\rangle$  corresponding to  $H^{eff}(t)$  can be established as:

$$|\Psi(t)\rangle = R(t) |\Phi(t)\rangle \quad (4)$$

## III. CONSTRUCTION OF THE ADIABATIC HAMILTONIAN

The next step of the analysis is to find the degenerate dark states (with null eigenvalues  $E_1 = E_2 = 0$  and zero components along the excited state  $|4\rangle$  of the effective Hamiltonian). In general, the N-pod systems have  $(N-1)$  dark states and 2 bright states. The dark states are:

$$|\phi_1(t)\rangle = \begin{pmatrix} \frac{\Omega_2(t)}{\chi_2(t)} \\ \frac{\Omega_3(t)}{\chi_3(t)} \\ 0 \\ 0 \end{pmatrix}, \quad |\phi_2(t)\rangle = \begin{pmatrix} \frac{\Omega_1(t)\Omega_3(t)}{\chi_2(t)\chi_3(t)} \\ \frac{\Omega_2(t)\Omega_3(t)}{\chi_2(t)\chi_3(t)} \\ \frac{\chi_2(t)}{\chi_3(t)} \\ 0 \end{pmatrix} \quad (5)$$

and the bright states corresponding to non-zero eigenvalues  $E_3 = +\chi_3/2, E_4 = -\chi_3/2$  are:

$$|\phi_3(t)\rangle = \begin{pmatrix} \frac{\Omega_1(t)}{\sqrt{2}\chi_3(t)} \\ \frac{\Omega_2(t)}{\sqrt{2}\chi_3(t)} \\ \frac{\Omega_3(t)}{\sqrt{2}\chi_3(t)} \\ -\frac{1}{\sqrt{2}} \end{pmatrix}, \quad |\phi_4(t)\rangle = \begin{pmatrix} \frac{\Omega_1(t)}{\sqrt{2}\chi_3(t)} \\ \frac{\Omega_2(t)}{\sqrt{2}\chi_3(t)} \\ \frac{\Omega_3(t)}{\sqrt{2}\chi_3(t)} \\ \frac{1}{\sqrt{2}} \end{pmatrix} \quad (6)$$

where,  $\chi_n^2 = \sum_{i=1}^n \Omega_i^2$ . To simplify, we can define new parameters, as:

$$\tan \vartheta_i = \frac{\Omega_{i+1}}{\chi_i} \quad i = 1, 2 \quad (7)$$

The angle  $\vartheta_1$  is the mixing angle used in standard STIRAP related to the pump,  $\Omega_1$ , and the Stokes,  $\Omega_2$ , pulses and  $\vartheta_2$  is additional mixing angle related to the control pulse,  $\Omega_3$ . The unitary transformation between the atomic bare states  $\{|1\rangle, |2\rangle, |3\rangle, |4\rangle\}$  and the adiabatic states  $\{|\phi_1\rangle, |\phi_2\rangle, |\phi_3\rangle, |\phi_4\rangle\}$ , which diagonalizes the effective Hamiltonian, is:

$$T(t) = \begin{pmatrix} \sin \vartheta_1 & \cos \vartheta_1 \sin \vartheta_2 & \frac{1}{\sqrt{2}} \cos \vartheta_1 \cos \vartheta_2 & \frac{1}{\sqrt{2}} \cos \vartheta_1 \cos \vartheta_2 \\ -\cos \vartheta_2 & \sin \vartheta_1 \sin \vartheta_2 & \frac{1}{\sqrt{2}} \sin \vartheta_1 \cos \vartheta_2 & \frac{1}{\sqrt{2}} \sin \vartheta_1 \cos \vartheta_2 \\ 0 & -\cos \vartheta_2 & \frac{1}{\sqrt{2}} \sin \vartheta_2 & \frac{1}{\sqrt{2}} \sin \vartheta_2 \\ 0 & 0 & -\frac{1}{\sqrt{2}} & \frac{1}{\sqrt{2}} \end{pmatrix} \quad (8)$$

The other form of transformation Eq. (8), in terms of Rabi frequencies, can be written as:

$$T(t) = \begin{pmatrix} \frac{\Omega_1 \Omega_2}{\chi_1 \chi_2} & \frac{\Omega_1 \Omega_3}{\chi_2 \chi_3} & \frac{1}{\sqrt{2}} \frac{\Omega_1}{\chi_3} & \frac{1}{\sqrt{2}} \frac{\Omega_1}{\chi_3} \\ -\frac{\chi_1}{\chi_2} & \frac{\Omega_2 \Omega_3}{\chi_2 \chi_3} & \frac{1}{\sqrt{2}} \frac{\Omega_2}{\chi_3} & \frac{1}{\sqrt{2}} \frac{\Omega_2}{\chi_3} \\ \chi_2 & \chi_2 \chi_3 & \frac{1}{\sqrt{2}} \frac{\Omega_3}{\chi_3} & \frac{1}{\sqrt{2}} \frac{\Omega_3}{\chi_3} \\ 0 & -\chi_2 & \frac{1}{\sqrt{2}} \frac{\Omega_3}{\chi_3} & \frac{1}{\sqrt{2}} \frac{\Omega_3}{\chi_3} \\ 0 & 0 & -\frac{1}{\sqrt{2}} & \frac{1}{\sqrt{2}} \end{pmatrix} \quad (9)$$

Hence, the Hamiltonian in the basis of adiabatic states can be written as:

$$H' = T^\dagger H^{\text{eff}} T - T^\dagger \frac{\partial T}{\partial t} \quad (10)$$

$$= \begin{pmatrix} 0 & -i \dot{\vartheta}_1 \sin \vartheta_2 & \frac{-i}{\sqrt{2}} \dot{\vartheta}_1 \cos \vartheta_2 & \frac{-i}{\sqrt{2}} \dot{\vartheta}_1 \cos \vartheta_2 \\ i \dot{\vartheta}_1 \sin \vartheta_2 & 0 & \frac{i}{\sqrt{2}} \dot{\vartheta}_2 & \frac{i}{\sqrt{2}} \dot{\vartheta}_2 \\ \frac{i}{\sqrt{2}} \dot{\vartheta}_1 \cos \vartheta_2 & -\frac{i}{\sqrt{2}} \dot{\vartheta}_2 & -\frac{1}{2} \chi_3 & 0 \\ \frac{i}{\sqrt{2}} \dot{\vartheta}_1 \cos \vartheta_2 & -\frac{i}{\sqrt{2}} \dot{\vartheta}_2 & 0 & +\frac{1}{2} \chi_3 \end{pmatrix}$$

The dynamics corresponding to  $H'(t)$  is given by  $i \frac{\partial}{\partial t} |\Phi'(t)\rangle = H'(t) |\Phi'(t)\rangle$ . The relation between  $|\Phi(t)\rangle$ , the state vector corresponding to  $H^{\text{eff}}(t)$ , and  $|\Phi'(t)\rangle$  is established by the unitary transformation  $T(t)$  as:

$$|\Phi(t)\rangle = T(t) |\Phi'(t)\rangle \quad (11)$$

In the adiabatic limit, which we have assumed to be applicable, the time derivative of the mixing angles  $\vartheta_1$ , and  $\vartheta_2$  is small compared to the splitting of the eigenvalues given by  $\chi_3/2$  (see Fig. 2). Under this condition, there is negligible non-adiabatic coupling of the adiabatic states,  $|\Phi_1(t)\rangle$  or  $|\Phi_2(t)\rangle$ , with the states of  $|\Phi_3(t)\rangle$  and  $|\Phi_4(t)\rangle$ .

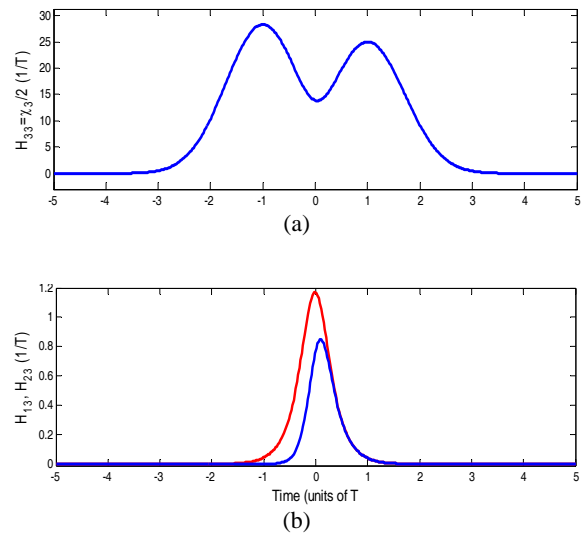


**Fig. 2** Comparison of the  $H'$  elements. There is a negligible nonadiabatic coupling of the adiabatic states,  $|\Phi_1(t)\rangle$  or  $|\Phi_2(t)\rangle$ , to the  $|\Phi_3(t)\rangle$  and  $|\Phi_4(t)\rangle$  states.

Therefore, in the adiabatic limit we must take into account only transitions between *degenerate* adiabatic dark states. This leads to:

$$H' = \begin{pmatrix} 0 & -i \dot{\vartheta}_1 \sin \vartheta_2 & 0 & 0 \\ i \dot{\vartheta}_1 \sin \vartheta_2 & 0 & 0 & 0 \\ 0 & 0 & -\frac{1}{2} \chi_3 & 0 \\ 0 & 0 & 0 & +\frac{1}{2} \chi_3 \end{pmatrix} \quad (12)$$

#### IV. TIME EVOLUTION OPERATOR IN THE ADIABATIC LIMIT

In the adiabatic limit, the time evolution operator corresponding to  $H^{ad}(t)$  can be written as:

$$U^{ad}(t, t_i) = e^{-i \int_{t_i}^t H^{ad}(s) ds} \quad (13)$$

Since  $H^{ad}$  has a block-diagonal structure,  $U^{ad}$  will be as:

$$U^{ad}(t, t_0) = \begin{pmatrix} U_g & 0 \\ 0 & U_d \end{pmatrix}, \quad (14.a)$$

$$U_g = \begin{pmatrix} \cos \gamma & -\sin \gamma \\ \sin \gamma & \cos \gamma \end{pmatrix}, \quad (14.b)$$

$$U_d = \begin{pmatrix} e^{-i\delta(t)} & 0 \\ 0 & e^{+i\delta(t)} \end{pmatrix}, \quad (14.c)$$

where,  $U_d, U_g$  are the dynamical and the geometrical blocks, respectively, and the dynamical and the geometrical phases,  $\gamma(t)$  and  $\delta(t)$  are respectively defined as:

$$\gamma(t) = \int_{t_i}^t \dot{\gamma}_1(s) \sin \vartheta_2(s) ds \quad (15.a)$$

$$\delta(t) = \frac{1}{2} \int_{t_i}^t ds \chi_3(s) \quad (15.b)$$

and  $U^{ad}(t, t_i)$  can be written as:

$$U^{ad}(t, t_i) = \begin{pmatrix} \cos \gamma(t) & -\sin \gamma(t) & 0 & 0 \\ \sin \gamma(t) & \cos \gamma(t) & 0 & 0 \\ 0 & 0 & e^{-i\delta(t)} & 0 \\ 0 & 0 & 0 & e^{+i\delta(t)} \end{pmatrix} \quad (16)$$

Considering, Eqs. (4), (10), (11), (13), we can write the state vector corresponding to  $H(t)$  as:

$$|\Psi(t)\rangle = R(t)T(t)U^{ad}(t, t_i)T^+(t_i)R^+(t_i)|\Psi(t_i)\rangle \quad (17)$$

This means that the time evolution operator corresponding to  $H(t)$  in adiabatic limit is:

$$U(t, t_i) = R(t)T(t)U^{ad}(t, t_i)T^+(t_i)R^+(t_i) \quad (18)$$

#### V. COHERENT POPULATION TRANSFER TO A SUPERPOSITION OF GROUND STATES

In this section, we divided our studies into three cases, with same initial state and different final states, at the end of the interaction.

##### A. Case 1

In this case, the goal is to transform the initial state of the system:

$$|\Psi(t_i)\rangle = |1\rangle = (1; 0; 0; 0)^T \quad (19.a)$$

at the end of interaction, into a ground state.

$$|\Psi(t_f)\rangle = |3\rangle = (0; 0; 1; 0)^T \quad (19.b)$$

Using Rabi frequencies of the fields as:

$$\lim_{t \rightarrow t_i} \frac{\Omega_1}{|\Omega_2|} \rightarrow 0, \quad (|\Omega_2| > |\Omega_3| > \Omega_1) \quad (20.a)$$

$$\lim_{t \rightarrow t_f} \frac{|\Omega_2|}{\Omega_1} \rightarrow 0, \quad (\Omega_1 > |\Omega_3| > |\Omega_2|) \quad (20.b)$$

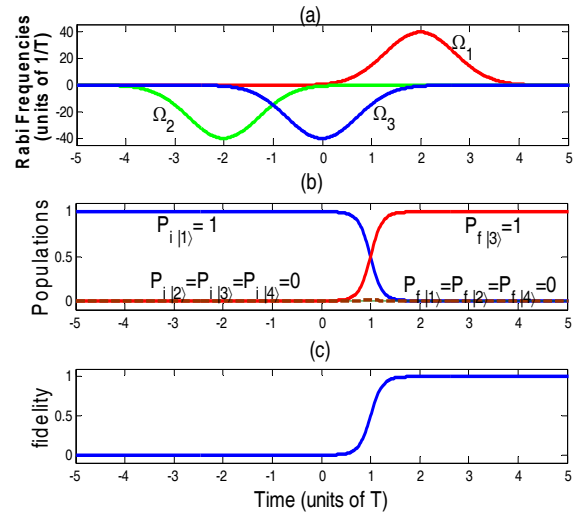


**Fig. 3** (a) Rabi frequencies of the laser fields with the Gaussian pulse parameters of  $\Omega_0 = 40/T$ ,  $\tau = 2T$ , (b) time evolution of the populations, and (c) dynamics of the fidelity of desired state (in case 1).

We have tried to transfer the initial population of the system, finally, to the desired state. By substituting, Eqs. (20) into Eq. (9), we will have:

$$T(t_i) = \begin{pmatrix} 1 & 0 & 0 & 0 \\ 0 & 0 & \frac{1}{\sqrt{2}} & \frac{1}{\sqrt{2}} \\ 0 & -1 & 0 & 0 \\ 0 & 0 & -\frac{1}{\sqrt{2}} & \frac{1}{\sqrt{2}} \end{pmatrix}, \quad (21.a)$$

$$T(t_f) = \begin{pmatrix} 0 & 0 & \frac{1}{\sqrt{2}} & \frac{1}{\sqrt{2}} \\ -1 & 0 & 0 & 0 \\ 0 & -1 & 0 & 0 \\ 0 & 0 & -\frac{1}{\sqrt{2}} & \frac{1}{\sqrt{2}} \end{pmatrix} \quad (21.b)$$

And substituting Eqs. (3), (16) and (21) into Eq. (18) gives:

$$U(t_f, t_i) = \begin{pmatrix} 0 & \cos\delta e^{+i(\theta_2 - \theta_1)} & 0 & -i\sin\delta \\ \cos\gamma e^{+i(\theta_1 - \theta_2)} & 0 & \sin\gamma e^{+i(\theta_3 - \theta_2)} & 0 \\ \sin\gamma e^{+i(\theta_2 - \theta_3)} & 0 & \cos\gamma & 0 \\ 0 & -i\sin\delta & 0 & \cos\delta \end{pmatrix} \quad (22)$$

Assuming,

$$\theta_1 = 0, \theta_2 = \theta_3 = \pi \quad (23)$$

Substituting Eq. (22) into Eq. (21) and applying the initial state of the system,  $|\Psi(t_i)\rangle$ , in Eq. (17) gives:

$$|\Psi(t_f)\rangle = U(t_f, t_i) |\Psi(t_i)\rangle = (0 \quad \cos\gamma \quad \sin\gamma \quad 0)^T \quad (24)$$

As it can be seen from Fig. 4, with  $\gamma = \pi/2$  and,  $\cos\delta = -1$ , the final state of the system at the end of the interaction transfer to:

$$|\Psi(t_f)\rangle = |3\rangle = (0 \quad 0 \quad 1 \quad 0)^T \quad (25)$$

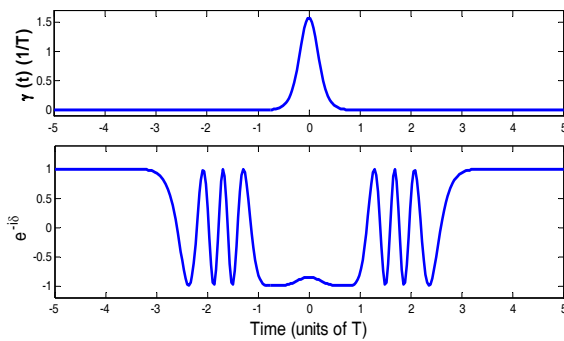


**Fig. 4** Geometrical phase (upper curve) and real part of  $\exp(-i\delta)$  (lower curve) for case 1, (Eq. (15)).

For a numerical analysis of the coherent population transfer to the desired state, we have assumed the Gaussian time-dependence of the Rabi frequencies, which are satisfied conditions of Eqs. (20) and (23), as:

$$\Omega_1(t) = \Omega_0 e^{-[(t-\tau)/T]^2} \quad (26.a)$$

$$\Omega_2(t) = -\Omega_0 e^{-[(t+\tau)/T]^2} \quad (26.b)$$

$$\Omega_3(t) = -\Omega_0 e^{-[(t-\tau)/T]^2} \quad (26.c)$$

where,  $\Omega_0, 2\tau, T$  are the peak Rabi frequency, the time delay between the pump and Stokes pulses and the pulse duration, respectively. The results are shown in Fig. 3. In Fig. 3.a, it is shown that the conditions of Eqs. (19) and (23) are satisfied with the Gaussian pulse parameters of  $|\Omega_{01}| = |\Omega_{02}| = |\Omega_{03}| = 40/T$  and  $\tau = 2T$ .

The time evaluation of the system populations is shown in Fig. 3.b, which represents a coherent superposition of ground states with final equal populations. The technique of adiabatic passage is also expected to be robust against the effects of the spontaneous emission, so, the excited atomic state  $|4\rangle$  is not populated in the adiabatic limit, in the all three cases studied here (this effect is denoted in Figures. 3.b, 5.b, and 7.b as  $P_f|4\rangle = 0$ ). The fidelity of the populations in different levels as a function of the time is shown in Fig. 3.c. It can be seen from Fig. 3.c that at  $t \rightarrow t_f$  fidelity of desired state at Eq. (24) is equal to one (%100).

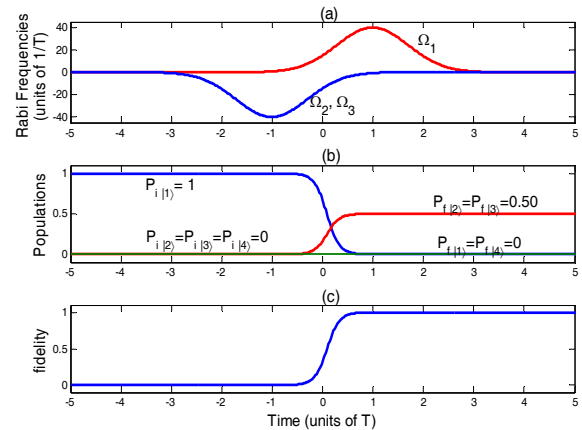


**Fig. 5** (a) Rabi frequencies of the laser fields with the Gaussian pulse parameters of  $\Omega_0 = 40/T$ ,  $\tau = 2T$ . (b) Time evolution of the populations, which represents a coherent superposition of the ground states with final equal populations. (c) Dynamics of the fidelity of desired state (in case 2.)

## B. Case 2

Another interesting case, that can be studied, is to transform the initial state of the system,

$$|\Psi(t_i)\rangle = |1\rangle = (1 \ 0 \ 0 \ 0)^T, \quad (27.a)$$

At the end of interaction, into a coherent superposition of other two ground states as:

$$|\Psi(t_f)\rangle = \frac{1}{\sqrt{2}}(|2\rangle + |3\rangle) \quad (27.b)$$

Using Rabi frequencies of the fields as:

$$\lim_{t \rightarrow t_i} \frac{\Omega_1}{|\Omega_2|} \rightarrow 0, \quad (|\Omega_2| = |\Omega_3| > \Omega_1) \quad (28.a)$$

$$\lim_{t \rightarrow t_f} \frac{|\Omega_2|}{\Omega_1} \rightarrow 0, \quad (\Omega_1 > |\Omega_3| = |\Omega_2|) \quad (28.b)$$

Substituting, Eqs. (28) into Eq. (9) gives:

$$T(t_i) = \begin{pmatrix} 1 & 0 & 0 & 0 \\ 0 & \frac{1}{\sqrt{2}} & \frac{1}{2} & \frac{1}{2} \\ 0 & -\frac{1}{\sqrt{2}} & \frac{1}{2} & \frac{1}{2} \\ 0 & 0 & -\frac{1}{\sqrt{2}} & \frac{1}{\sqrt{2}} \end{pmatrix}, \quad (29.a)$$

$$T(t_f) = \begin{pmatrix} 0 & 0 & \frac{1}{\sqrt{2}} & \frac{1}{\sqrt{2}} \\ -1 & 0 & 0 & 0 \\ 0 & -1 & 0 & 0 \\ 0 & 0 & -\frac{1}{\sqrt{2}} & \frac{1}{\sqrt{2}} \end{pmatrix} \quad (29.b)$$

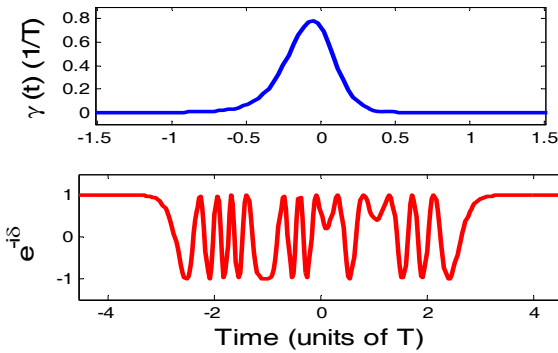


**Fig. 6** Geometrical phase (upper curve) and real part of  $\exp(-i\delta)$  (lower curve) for case 2, (Eq. (15)).

Then, substituting Eqs. (3), (16) and (29) into Eq. (18) gives:

$$U(t_f, t_i) = \begin{pmatrix} 0 & \frac{1}{\sqrt{2}} \cos \delta e^{+i(\theta_2 - \theta_1)} & \frac{1}{\sqrt{2}} \cos \delta e^{+i(\theta_3 - \theta_1)} & -i \sin \delta \\ -\cos \gamma e^{+i(\theta_1 - \theta_2)} & \frac{1}{\sqrt{2}} \sin \gamma & \sin \gamma e^{+i(\theta_3 - \theta_2)} & 0 \\ -\sin \gamma e^{+i(\theta_1 - \theta_3)} & -\frac{1}{\sqrt{2}} \cos \gamma e^{+i(\theta_2 - \theta_3)} & \cos \gamma & 0 \\ 0 & -\frac{i}{\sqrt{2}} \sin \delta & -\frac{i}{\sqrt{2}} \sin \delta & \cos \delta \end{pmatrix} \quad (30)$$

Finally, by substituting Eq. (23) into Eq. (30), and the initial state of the system, Eq. (27a), into Eq. (17), the vector of state is become:

$$|\Psi(t_f)\rangle = U(t_f, t_i) |\Psi(t_i)\rangle = (0 \ \cos \gamma \ \sin \gamma \ 0)^T \quad (31)$$

As it can be seen from Fig. 6, with  $\gamma = \pi/4$  and,  $\cos \delta = -1$ , the final state of the system, at the end of the interaction, is transferred to:

$$|\Psi(t_f)\rangle = \frac{1}{\sqrt{2}}(0 \ 1 \ 1 \ 0)^T \quad (32)$$

For a numerical analysis of the coherent population transferring of the system to the desired state, we have assumed the Gaussian time-dependence of the Rabi frequencies, which are satisfied condition of Eqs. (28) and (23), as:

$$\Omega_1(t) = \Omega_0 e^{-[(t-\tau)/T]^2} \quad (33.a)$$

$$\Omega_2(t) = \Omega_3(t) = -\Omega_0 e^{-[(t+\tau)/T]^2} \quad (33.b)$$

The results are shown in Fig. 5. It is shown in Fig. 5.a that the conditions of Eqs. (27) and (23) are satisfied with the Gaussian pulse parameters of  $|\Omega_{01}| = |\Omega_{02}| = |\Omega_{03}| = 40/T$  and  $\tau = 2T$ . The time evaluations of the system populations are shown in Fig. 5.b, which represents a coherent superposition of the ground states with final equal populations. The fidelity of the populations in different levels as functions of time is shown in Fig. 5.c. It can be seen from Fig. 5.c that at  $t \rightarrow t_f$  fidelity of desired state at Eq. (31) is equal to one (%100).

## C. Case 3

The other interesting case that can be studied is to transform the initial state of the system:

$$|\Psi(t_i)\rangle = |1\rangle, \quad (34.a)$$

at the end of interaction, into a coherent superposition of other two ground states as:

$$|\Psi(t_f)\rangle = \frac{1}{\sqrt{3}}(|1\rangle + |2\rangle + |3\rangle) \quad (34.b)$$

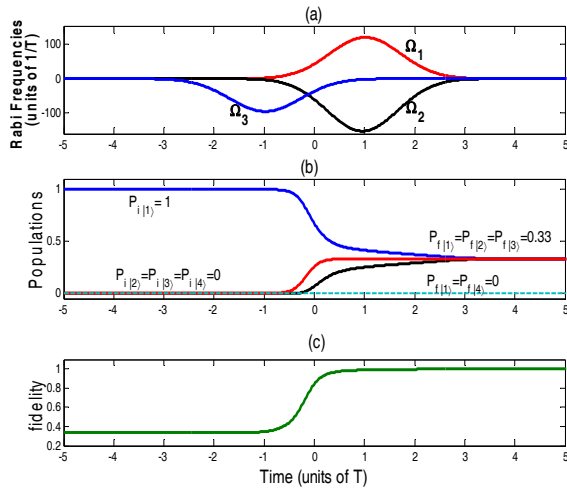


**Fig. 7** (a) Rabi frequencies of the laser fields with the Gaussian pulse parameters of  $\Omega_{10}=120/T$ ,  $\Omega_{20}=150/T$ ,  $\Omega_{30}=120/T$ , and  $\tau=2T$ , (b) time evolution of the populations, which represents a coherent superposition of the ground states with final equal populations, and (c) dynamics of the fidelity of desired state (in case 3).

Using Rabi frequencies of the fields as:

$$\lim_{t \rightarrow t_i} \frac{\Omega_1}{|\Omega_2|} \rightarrow 0, (|\Omega_3| > |\Omega_2| = \Omega_1) \quad (35.a)$$

$$\lim_{t \rightarrow t_f} \frac{|\Omega_2|}{\Omega_1} \rightarrow 0, (\Omega_1 = |\Omega_2| > |\Omega_3|) \quad (35.b)$$

The unitary transformation,  $T(t)$ , at the initial and final times of the interaction, can be found by replacing Eqs. (35) into Eq. (9) as:

$$T(t_i) = \begin{pmatrix} 1/\sqrt{2} & 1/\sqrt{2} & 0 & 0 \\ -1/\sqrt{2} & 1/\sqrt{2} & 0 & 0 \\ 0 & 0 & 1/\sqrt{2} & 1/\sqrt{2} \\ 0 & 0 & -1/\sqrt{2} & 1/\sqrt{2} \end{pmatrix} \quad (36.a)$$

$$T(t_f) = \begin{pmatrix} 1/\sqrt{2} & 0 & 1/2 & 1/2 \\ -1/\sqrt{2} & 0 & 1/2 & 1/2 \\ 0 & -1 & 0 & 0 \\ 0 & 0 & -1/\sqrt{2} & 1/\sqrt{2} \end{pmatrix} \quad (36.b)$$

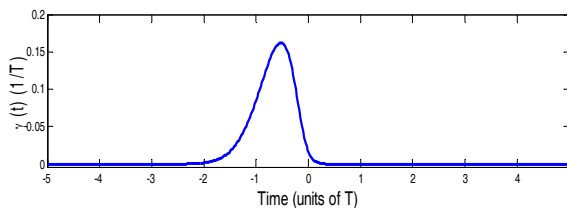


**Fig. 8** Geometrical phase for case 3 (Eq. (15a)).

And, by substituting Eqs. (3), (16), and (36) into Eq. (18), the time evaluation operator can be found as:

$$U(t, t_i) = \begin{pmatrix} \frac{1}{2}(\cos\gamma - \sin\gamma) & -\frac{1}{\sqrt{2}}(\cos\gamma + \sin\gamma)e^{+i(\theta_2 - \theta_1)} \\ -\frac{1}{2}(\cos\gamma - \sin\gamma)e^{+i(\theta_1 - \theta_2)} & \frac{1}{2}(\cos\gamma + \sin\gamma) \\ -\frac{1}{\sqrt{2}}(\cos\gamma + \sin\gamma)e^{+i(\theta_1 - \theta_2)} & -\frac{1}{\sqrt{2}}(\cos\gamma - \sin\gamma)e^{+i(\theta_2 - \theta_1)} \\ 0 & 0 \end{pmatrix} \quad (37)$$

$$\begin{pmatrix} \frac{1}{\sqrt{2}}\cos\delta e^{+i(\theta_3 - \theta_1)} & -\frac{i}{\sqrt{2}}\sin\delta \\ \frac{1}{\sqrt{2}}\cos\delta e^{+i(\theta_3 - \theta_2)} & -\frac{i}{\sqrt{2}}\sin\delta \\ 0 & 0 \\ -i\sin\delta & \cos\delta \end{pmatrix}$$

Finally, by substituting Eq. (23) into Eq. (37), and the initial state of the system, Eq. (34a), into Eq. (17) the vector state of the system at the end of the evolution, can be written as:

$$|\Psi(t_f)\rangle = U(t_f, t_i) \begin{pmatrix} 1 \\ 0 \\ 0 \\ 0 \end{pmatrix} = \begin{pmatrix} \frac{1}{2}(\cos\gamma - \sin\gamma) \\ \frac{1}{2}(\cos\gamma - \sin\gamma) \\ \frac{1}{\sqrt{2}}(\cos\gamma + \sin\gamma) \\ 0 \end{pmatrix} \quad (38)$$

As it can be seen from Fig. 8, with  $\gamma = -0.17 \text{ Rad}$  and  $\cos\delta = -1$ , the final state of the system at the end of the interaction is transferred to:

$$|\Psi(t_f)\rangle = \frac{1}{\sqrt{3}}(1 \ 1 \ 1 \ 0)^T \quad (39)$$

For a numerical analysis of the coherent population transfer to the desired state, we have assumed the Gaussian time-dependence of the Rabi frequencies which are satisfied the conditions of Eqs. (35) and (23), as:

$$\Omega_1(t) = \Omega_0 e^{-[(t-1.1\tau)/T]^2} \quad (40.a)$$

$$\Omega_2(t) = 1.27\Omega_0 e^{-[(t-0.97\tau)/T]^2} \quad (40.b)$$

$$\Omega_3(t) = 0.8\Omega_0 e^{-[(t+0.97\tau)/T]^2} \quad (40.c)$$

The results are shown in Fig. 7. It is shown in Fig. 7.a that the conditions of Eqs. (34) and (23) are satisfied with the Gaussian pulse parameters of  $|\Omega_{01}| = |\Omega_{02}| = |\Omega_{03}| = 40/T$  and  $\tau = 2T$ .

The time evolutions of the system populations are shown in Fig. 7.b, which represents a coherent superposition of ground states with



final equal populations. The fidelity of the populations, in different levels, as a function of time is shown in Fig. 7.c. It can be seen from Fig. 7.c that at  $t \rightarrow t_f$  fidelity of desired state at Eq. (38) is equal to one (%100).

## VI. IMPLEMENTATION OF THE SINGLE-QUTRIT QUANTUM GATE VIA TRIPOD ADIABATIC PASSAGE

With  $\gamma = \pi/2$  and  $\cos \delta = -1$ , in Eq. (22) and under the conditions of Eqs. (20) and (23), the single-qutrit quantum gate is resulted, via tripod adiabatic passage, as:

$$U_{3 \times 3} = \begin{pmatrix} 0 & 1 & 0 \\ 0 & 0 & 1 \\ 1 & 0 & 0 \end{pmatrix} \quad (41)$$

Similarly, to transform the initial state of the system  $|\Psi(t_i)\rangle = |1\rangle = (1;0;0;0)^T$ , at the end of interaction, into a ground state  $|\Psi(t_f)\rangle = |2\rangle = (0;1;0;0)^T$ , the single-qutrit quantum gate can be obtained as:

$$U_{3 \times 3} = \begin{pmatrix} 0 & 1 & 0 \\ 1 & 0 & 0 \\ 0 & 0 & 1 \end{pmatrix} \quad (42)$$

With  $\gamma = \pi/4$  and  $\cos \delta = -1$  in Eqs. (30), and with the use of Eqs. (28) and (23), the other single-qutrit quantum gate is obtained via tripod adiabatic passage, as follows:

$$U_{3 \times 3} = \frac{1}{\sqrt{2}} \begin{pmatrix} 0 & 1 & 1 \\ 1 & \frac{1}{\sqrt{2}} & \frac{1}{\sqrt{2}} \\ 1 & \frac{1}{\sqrt{2}} & \frac{1}{\sqrt{2}} \end{pmatrix} \quad (43)$$

Also, to transform the initial state of the system  $|\Psi(t_i)\rangle = |2\rangle = (0;1;0;0)^T$ , at the end of interaction, into the superposition of the ground states  $|\Psi(t_f)\rangle = \frac{1}{\sqrt{2}}(|1\rangle + |3\rangle)$ , the single-qutrit quantum gate can be obtained as:

$$U_{3 \times 3} = \frac{1}{\sqrt{2}} \begin{pmatrix} \frac{1}{\sqrt{2}} & 1 & \frac{1}{\sqrt{2}} \\ 1 & 0 & 1 \\ \frac{1}{\sqrt{2}} & 1 & \frac{1}{\sqrt{2}} \end{pmatrix} \quad (44)$$

For obtaining another single-qutrit quantum gate, we were replaced  $\gamma = -0.17$  and  $\cos \delta = -1$  in Eq. (37), and used the conditions given in Eqs. (23), and found:

$$U_{3 \times 3} = \frac{1}{\sqrt{6}} \begin{pmatrix} \sqrt{2} & 1 & \sqrt{3} \\ \sqrt{2} & 1 & \sqrt{3} \\ \sqrt{2} & 2 & 0 \end{pmatrix} \quad (45)$$

As the upper ways, to transform the initial state of the system  $|\Psi(t_i)\rangle = |2\rangle = (0;1;0;0)^T$ , at the end of interaction, into the superposition of the ground states  $|\Psi(t_f)\rangle = \frac{1}{\sqrt{2}}(|1\rangle + |2\rangle + |3\rangle)$ , the single-qutrit quantum gate can be found as:

$$U_{3 \times 3} = \frac{1}{\sqrt{6}} \begin{pmatrix} 1 & \sqrt{2} & \sqrt{3} \\ 1 & \sqrt{2} & \sqrt{3} \\ 2 & \sqrt{2} & 0 \end{pmatrix} \quad (46)$$

## VII. CONCLUSION

We have studied stimulated Raman adiabatic passage in tripod configurations by deriving the corresponding propagator in adiabatic limit. We emphasize the presence of non-Abelian geometrical phase in propagator, which can be controlled by an appropriate time delay and peak amplitude ratios of the pulses. A proper time scaling of the Rabi frequencies allows us to transfer the population of the system to a desired superposition of ground states with the highest fidelity. In this paper, we also obtained and implemented the single-qutrit unitary gates. The presented analytical solutions and numerical results can be generalized to N-pod systems which have a significant potential for creation multi-atom entanglement and implementation multi-bit unitary gates.

## REFERENCES

- [1] M. A. Nielsen and I. L. Chuang, *Quantum Computation and Quantum Information*, Cambridge University Press, Cambridge, 2000.



- [2] D. Bouwmeester, A. Ekert, and A. Zeilinger, *The physics of Quantum Information*, Springer, Berlin, 2000.
- [3] E. S. Kyoseva and N. V. Vitanov, "Coherent pulsed excitation of degenerate multistate systems: exact analytic solutions," *Phys. Rev. A*, Vol. 73, pp. 023420 (1-9), 2006.
- [4] Y. B. Zhan, L. L. Zhang, and Q. Y. Zhang, "Quantum secure direct communication by entangled qutrits and entanglement swapping," *Opt. Commun.*, Vol. 282, pp. 4633-4636, 2009.
- [5] Z. Kis and F. Renzoni, "Qutrit rotation by stimulated Raman adiabatic passage" *Phys. Rev. A*, Vol. 65, pp. 032318 (1-4), 2002.
- [6] A. Galindo and M. A. Martin-Delgado, "Classical and quantum information and computation," *Rev. Mod. Phys.*, Vol. 74, pp. 383-389, 2002.
- [7] N. Vitanov, T. Halfmann, B. W. Shore, and K. Bergmann, "Laser-induced population transfer by adiabatic passage techniques," *Ann. Rev. Phys. Chem.* Vol. 52, pp. 763-768, 2001.
- [8] R. G. Unanyan, M. Fleischhauer, B. W. Shore, and K. Bergmann "Robust creation and phase-sensitive probing of superposition states via stimulated Raman adiabatic passage STIRAP with degenerate dark states," *Opt. Commun.*, Vol. 155, pp. 144-149, 1998.
- [9] R. G. Unanyan, B. W. Shore, and K. Bergmann, "Laser-driven population transfer in four-level atoms: Consequences of non-Abelian geometrical Adiabatic phase factors," *Phys. Rev. A*, Vol. 59, pp. 2910-2919, 1999.

THIS PAGE IS INTENTIONALLY LEFT BLANK.